Desalination and Water Treatment
www.deswater.com

doi: 10.5004/dwt.2017.20472

70 (2017) 261–268
April

Procedure optimization for removal of 2,4-dichlorophenoxyacetic acid from water by surfactant-modified magnetic nanoparticles

Seied Mahdi Pourmortazavi[a,*], Mehdi Taghdiri[b,c], Razieh Ahmadi[b], Mir Mahdi Zahedi[d]

[a]*Faculty of Material and Manufacturing Technologies, Malek Ashtar University of Technology, Tehran, Iran, Fax: +98-212-2936578; email: pourmortazavi@yahoo.com*
[b]*Department of Chemistry, Payame Noor University, PO Box 19395-3697, Tehran, Iran, emails: taghdiri@pnu.ac.ir (M. Taghdiri), razieh_ahmadi20@yahoo.com (R. Ahmadi)*
[c]*Research Center of Environmental Chemistry, Payame Noor University, Ardakan, Yazd, Iran*
[d]*Department of Marine Chemistry, Faculty of Marine Sciences, Chabahar Maritime University, Chabahar, Iran, email: idm.m.zahedi@gmail.com*

Received 14 June 2016; Accepted 27 December 2016

ABSTRACT

In this investigation, operation conditions of the separation procedure were optimized for efficient removal of 2,4-dichlorophenoxyacetic acid (2,4-D) from water by adsorption on the surface of Fe_3O_4 magnetic nanoparticles (MNPs) modified with cethyl trimethyl ammonium bromide (CTAB). In this order, Fe_3O_4 MNPs with the average size of about 60 nm were synthesized and characterized by scanning electron microscopy and infrared techniques. The surface of the nanoparticles was modified by coating with 3-(trimethoxysilyl)-1-porpanethiol and CTAB, respectively. Then, the modified MNPs were utilized to remove 2,4-D from the polluted water. The results of process optimization showed that at pH 9, temperature of 20°C, CTAB amount of 300 mg mL^{-1}, salt amount of 0.01 M and contact time of 30 min, maximum removal yield could be achieved. The study of the process kinetic showed that 2,4-D removal take places during a rapid sorption via a pseudo-second-order model. Thus, 2,4-D adsorption equilibrium data was fitted well, and the maximum monolayer capacity (q_{max}) was calculated as 4.9 mg g^{-1}.

Keywords: Fe_3O_4–TMSPT; Magnetic nanoparticles; CTAB coating; 2,4-dichlorophenoxyacetic acid; 2,4-D; Pollution removal

1. Introduction

An important problem in the modern world is treatment and removal of the environmental pollutions. 2,4-dichlorophenoxyacetic acid (with the commercial name of 2,4-D) is belonging to the phenoxy alkanoic acid herbicides. This herbicide is widely utilized for the post-emergence inhibition of different leaf weeds in forests, grain croplands, commercial turfs, and also aquacultures [1]. Utilizing 2,4-D in the agriculture leads to the presence of 2,4-D in the environments with consequent unfavorable effects in the ecosystems. 2,4-D is a water soluble substance and survives in the aqueous solutions as two different forms of neutral and anionic. 2,4-D commonly might be found in the anionic form at the pH range of the natural environment, because this herbicide has a low acidity (p*Ka* = 2.73) [2]. The anionic 2,4-D contaminant has high mobility and poor biodegradability [3]. Values of lethal dose in 50% of the treated animals (LD_{50}) for 2,4-D range from 639 to 1,646 mg kg^{-1} in the rats depending on the chemical form of 2,4-D used in the investigations [4]. The half-life of this pollutant in water varies from one to several weeks under the aerobic conditions, while this time might be longitude to 120 d under the anaerobic conditions [4]. Due to the high mobility and toxicity of the 2,4-D, it diffuses to the surface water and groundwater sources, and hence, this compound is among the major contaminants of the environment [5]. Therefore, the development of new adsorbents to

* Corresponding author.

efficient and cost-effective removal of the 2,4-D from water is interesting.

Adsorption in terms of initial cost, simple design and facile operation is a superior route in comparison with other techniques in order to remove odor, colors, oils, and also organic pollutants from waste effluents [6]. Until today, different routes have been proposed to develop the efficient adsorbents for removal of 2,4-D from water samples. These approaches include the use of biopolymers based on chitin and chitosan [7], organometallic framework [8], modified nanofibers by cations of *N*-cetylpyridinium [9], carbon cloth with high area [10], MIEX resin [11], double hydroxide of layered Cu–Fe [12], maize cob shape carbon [13], mesoporous carbons templated by SBA-15 [14], and bituminous shale [15], while further efforts to achieve the more efficient adsorbents are still ongoing.

Now a days, nanostructured materials have obtained a great interest and importance in separation and purification applications [16,17]. Nanomaterials commonly possess low densities and high specific surfaces, which make them appropriate candidates for utilization as the sorbent [18–20]. Meanwhile, nanomaterials with magnetic properties are interested for utilizing in different fields of science and technology. Separation techniques based on magnetic operation are attractive in separation science [21,22] due to the possibility of facile recovery of adsorbent from the separation solutions via application of an external magnetic field. This property makes MNPs principally appropriate for sample preparation since no centrifugation or filtration of sample is required after extraction. In fact, Fe_3O_4 nanoparticles are respectable candidate for magnetic carrier technology in view of the following main advantages: (1) these nanoparticles could be fabricated in large scales using a simple method; (2) the MNPs have high adsorption capacity with respect to their large surface area; and (3) these nanoparticles have low toxicity and strong magnetic properties. These magnetic adsorptives have been utilized widely for removal or concentration of various compounds, i.e., metal ions [23,24], herbicides and pesticides [25,26], and also gaseous materials [27] from different solutions. Up to date, extensive investigation has been carried out on the magnetic iron oxide nanoparticles as an attractive adsorbent, which possesses large surface area and small diffusion resistance during the separation steps. The main goal of the present study was the investigation about the removal of 2,4-D from water solution by synthesized Fe_3O_4 magnetic nanoparticles (MNPs) modified with cethyl trimethyl ammonium bromide (CTAB). To the best of our knowledge, there is no report on the removal of 2,4-D by Fe_3O_4 MNPs.

2. Experimental setup

2.1. Instrumentation

A pH-meter of Metrohm 691 (Herisau, Switzerland) was utilized for the pH measurements. A Cintra 6 spectrophotometer (GBC company from Australia) was applied for determining 2,4-D in aqueous solutions. Infrared (IR) spectra were recorded on an Fourier transform infrared spectrometer Shimadzu model Prestige-21 (Japan). A Heidolph heater-stirrer and ultrasonic bath of SonoSwiss model SW6H were utilized in the synthesis of MNPs, while a mechanical stirrer was utilized for separation operations. Scanning electron microscopy (SEM) was carried out by KYKY model EM3200 (China) to confirm the morphology of the synthesized and coated MNPs. Zeiss EM900 TEM was applied for transmission electron microscopy (TEM), while the samples were coated on a Cu grid covered with a layer of carbon. MNPs were captured from separation media by a neodymium iron boron magnet of 1.2 T after finishing of the adsorption.

2.2. Reagents

All chemicals and reagents, i.e., ferric chloride ($FeCl_3.6H_2O$), ferrous chloride ($FeCl_2.4H_2O$), CTAB, 3-(trimethoxysilyl)-1-porpanethiol (TMSPT), with the chemical structure shown in Fig. 1(a), were of analytical grade purchased from Merck (Darmstadt, Germany). 2,4-D was purchased from Sigma-Aldrich (Poole, Dorset, UK), and its stock solution was prepared using deionized water. Also, other utilized chemicals including ammonia, sodium citrate, glycerol, sodium chloride, ethanol, nitric acid, and hydrochloric acid were purchased from Merck (Darmstadt, Germany) and used as received.

2.3. Preparation of coated Fe_3O_4 magnetic NPs

MNPs were prepared via an improved chemical coprecipitation route [28]. At the first stage, aqueous solutions of $FeCl_2.4H_2O$ (2.15 g of salt dissolved in 50 mL deionized water) and $FeCl_3{\cdot}6H_2O$ (5.48 g of salt dissolved in 50 mL deionized water) were transferred into a 250-mL round-bottom flask while stirred at 85°C under nitrogen atmosphere. In the next step, 20 mL of 25% aqueous ammonia gradually were introduced to the solution that causes changing the color of solution (from orange to black). Then, the solution was cooled, and the resulted magnetic precipitate was separated via neodymium iron boron magnet. The collected precipitate was washed with deionized water and 100 mL of 0.02 M sodium chloride, respectively. In order to surface protection and modification

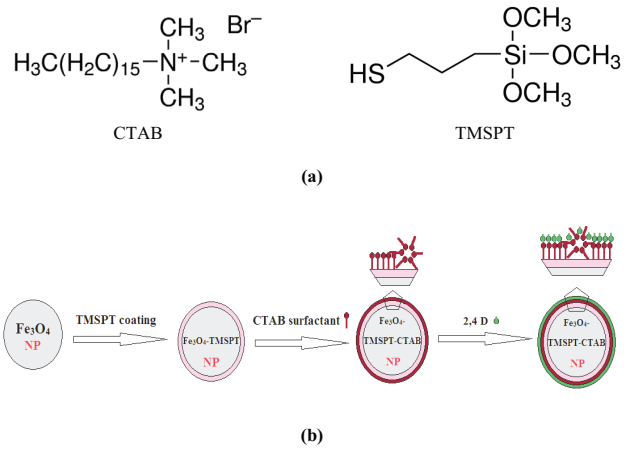

Fig. 1. (a) Chemical structure of cethyl trimethyl ammonium bromide (CTAB) and 3-(trimethoxysilyl)-1-porpanethiol (TMSPT) and (b) Scheme of the magnetic nanoparticles (MNPs) synthesis and 2,4-dichlorophenoxyacetic acid (2,4-D) removal process.

of the prepared MNPs, their surface at first was coated by TMSPT. Thus, the MNPs were treated by introducing 40 mL aqueous solution of TMSPT (10%, v/v) and then 30 mL of glycerol besides refluxing at the temperature of 90°C during 2 h. The resulted particles were removed from the solution by the magnet and washed two times with 100 mL water and methanol, respectively. In order to activate the surface of the coated MNPs, they were suspended in 100 mL and treated at first with 20 mL aqueous solution of sodium citrate (0.1 M) under nitrogen atmosphere and room temperature during 30 min, while the solution stirred vigorously, then the solution was subjected to the ultrasonic bath at 60°C for 15 min. Thereafter, the solution of the resulted suspended nanoparticles were mixed with CTAB solution (with the ratio of 1:1 (v/v)), stirred with 40 rpm for 30 min and then kept constant at room temperature for 12 h. Fig. 1(b) schematically shows the NPs synthesis and 2,4-D removing processes.

2.4. Optimization of 2,4-dichlorophenoxyacetic acid adsorption

Adsorption procedure of 2,4-D was accomplished by interaction of CTAB-coated Fe_3O_4 MNP (0.18 mg) with 18 mL aqueous solution of 100 ppm 2,4-D at suitable pH and salt amount during 10 min on the stirrer (80 rpm). The resulted solid phase was separated using 1.2 T neodymium iron boron magnet. Spectrophotometric absorbance of 2,4-D in residual feed aqueous solution was used to determine the yield of removal via a suitable calibration curve and applying following equation. Fig. 2 illustrates UV–Vis spectrum of 2,4-D in aqueous media.

$$\%2,4-\mathrm{D\,adsorption}=\left(\frac{C_i-C_r}{C_i}\right)\times 100 \tag{1}$$

where C_i and C_r are, respectively, initial and residual 2,4-D concentration (mg L^{-1}). To achieve maximum efficiency of 2,4-D removal from aqueous solution, various effective parameters including pH, temperature, time, amounts of coated CTAB, MNPs, and NaCl were studied and optimized.

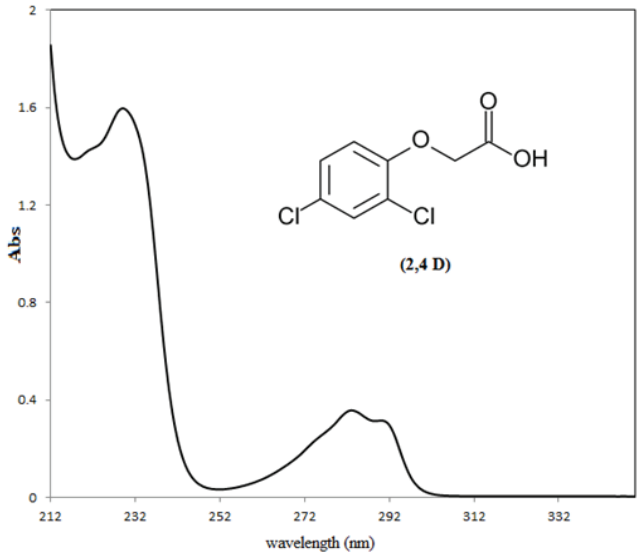

Fig. 2. UV–Vis spectrum of 2,4-D dissolved in water (30 ppm).

2.5. Mathematical modeling and kinetic studies of 2,4-D adsorption

The equilibrium isotherm equations are useful to describe the experimental sorption data. Commonly Langmuir, Freundlich, and Toth isotherms are utilized for describing the solid–liquid sorption systems [29]. The isotherms and kinetic models were utilized to describe the sorption data resulted from 2,4-D sorption. The isotherm and kinetic models parameters for 2,4-D were computed via non-linear error functions minimizing by the aid of solver add-in with Microsoft's spreadsheet, Excel. Chi-square statistic was utilized to assess the fitness of the isotherms and kinetic equations to 2,4-D experimental data. The Chi-square test statistic is the sum of the squares resulted from the differences between the experimental data and the calculated data by models. The corresponding mathematical statement for these parameters is as follows:

$$\chi^2=\sum_{i=1}^{N}\frac{(q_{e,\mathrm{exp.}}-q_{e,\mathrm{calc.}})^2}{q_{e,\mathrm{calc.}}} \tag{2}$$

where $q_{e,\mathrm{exp.}}$ and $q_{e,\mathrm{calc.}}$ are the values of equilibrium capacity resulted from the experimental data and calculated by the model in mg g^{-1}, respectively. Similarity of the model result and the experimental data leads to the small number for χ^2, while considerable difference of model and experimental data yields a large number for χ^2.

3. Results and discussion

3.1. MNPs preparation and characterization

Fig. 3 gives the SEM picture of the prepared Fe_3O_4 nanoparticles. As seen in Fig. 3(a), the prepared MNPs have a spherical morphology with average diameter of about 60 nm. Fig. 3(b) shows the SEM picture of MNPs coated with TMSPT while the particles have an average particle size similar to the previous image without further agglomeration of the particles. On the other hand, Fig. 3(c) displays the SEM image of MNPs–TMSPT modified with CTAB. As could be seen, the resulted nanoparticles have an average diameter of about 60 nm without further agglomeration with respect to the initial nanoparticles (MNPs before coating). Also, Fig. 3(d) displays the TEM image of MNPs–TMSPT modified with CTAB. As seen, this image confirms the SEM result and shows the resulted nanoparticles possess an average diameter of 60 nm. The obtained Fe_3O_4 nanoparticles were characterized by X-ray powder diffraction (XRD) to assess their structure and chemical composition [30,31]. The resulted XRD pattern is displayed in Fig. 4. As could be seen, all diffraction peaks indexed in the obtained pattern are consistent with the magnetite form of iron oxide (according to JCPDS 98-011-1283, diffraction software). Fig. 5 shows -IR spectrum of Fe_3O_4 nanoparticles before and after coating with TMSPT and also MNPs–TMSPT modified with CTAB. Fig. 5(a) presents the IR spectrum for the prepared MNPs before and after coating with TMSPT. As seen, two peaks are observed at 443 and 580 cm^{-1} corresponding to the stretching of Fe^{+2} and Fe^{+3} bonds with oxygen atom. The peak at 1,672 cm^{-1} is attributed to the stretching and bending vibrations of the adsorbed nitrogen at the surface of nanoparticles, while the wide peak

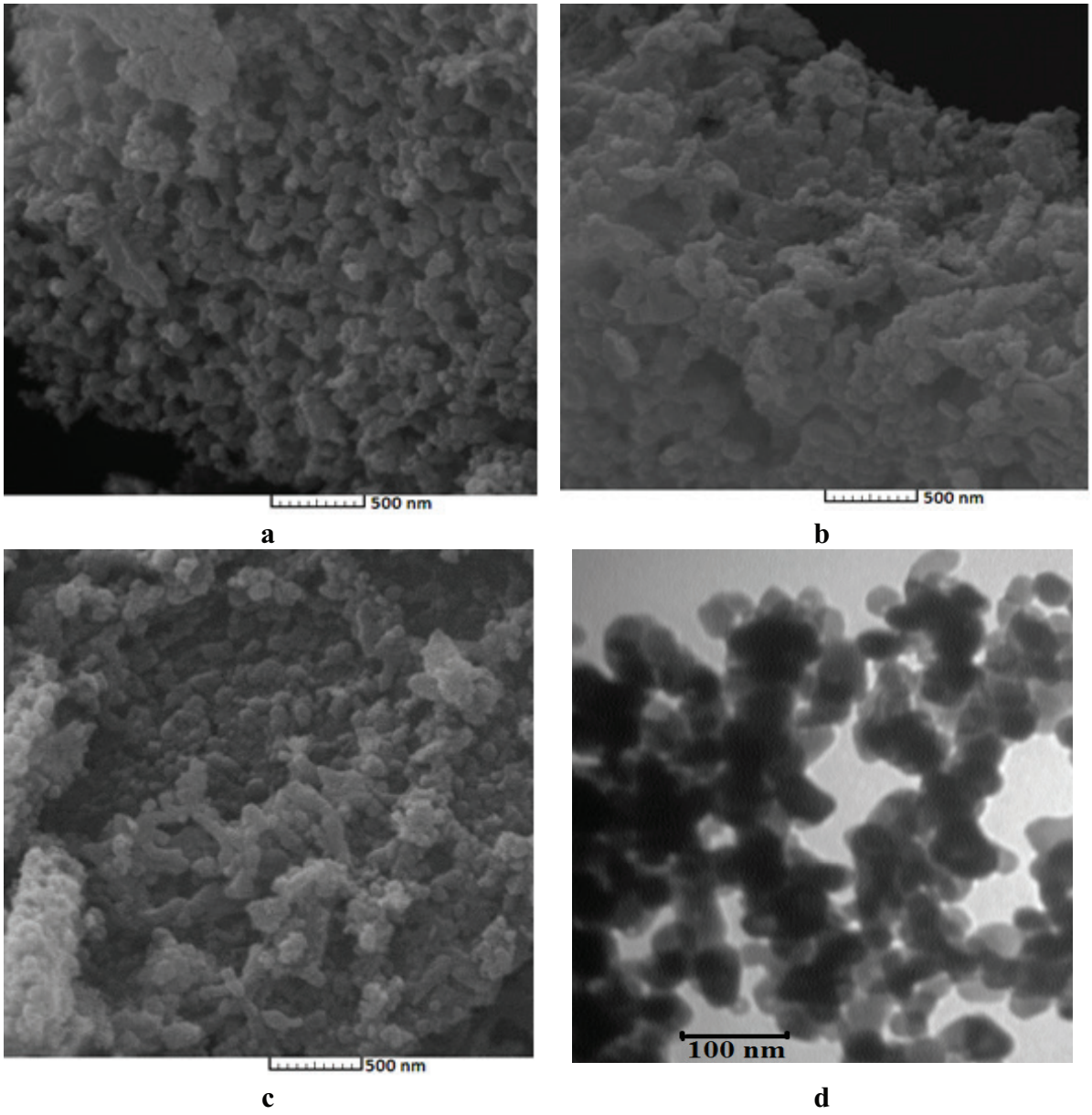

Fig. 3. SEM images of (a) synthesized Fe_3O_4 nanoparticles; (b) Fe_3O_4–TMSPT nanoparticles; (c) Fe_3O_4–TMSPT nanoparticles modified with CTAB; and (d) TEM images of Fe_3O_4–TMSPT nanoparticles modified with CTAB.

at 3,392 cm^{-1} is responsible for the vibration of hydroxyl group of the water. The IR spectrum of the MNPs coated with TMSPT shows some new peaks. The appeared peaks at 1,035 and 1,116 cm^{-1} are responsible for stretching vibrations of Si–O–Si bonds, and the peaks at 2,854 and 2,924 cm^{-1} are attributed to the stretching vibrations of C–H and S–H bonds of TMSPT molecules. Fig. 5(b) presents the IR spectrum of the MNPs–TMSPT modified with CTAB. The new peak appeared at 2,922 cm^{-1} is responsible for stretching vibrations of C–H bonds, and the peak at 2,500 cm^{-1} is attributed to the stretching vibrations of C–N bonds of amine in the structure of CTAB molecules. As expected the peaks corresponding to the CTAB are very weak in comparison with the MNPs and TMSPT because only small amount of surfactant is adsorbed on the surface of particles and hence its concentration in the KBr tablet is very low.

3.2. Effects of pH on adsorption of 2,4-dichlorophenoxyacetic acid

The presence of the active protons in the 2,4-D molecule caused the pH of solution has a strong effect on the adsorption procedure. The effect of pH on the adsorption of 2,4-D (in a solution with the concentration of 33 ppm) was investigated at the pH range of 2–12, while the other

variables, i.e., amounts of MNP (0.18 g), CTAB (65 ppm), NaCl salt (0.01 M), temperature (20°C), and time (10 min) were kept constant. The results shown in Fig. 6 display that the maximum 2,4-D adsorption was occurred at pH of 9. Observing this trend suggests that the adsorbed 2,4-D molecules are in anionic state and the electrostatic interactions between CTAB and 2,4-D molecules are important in the adsorption process.

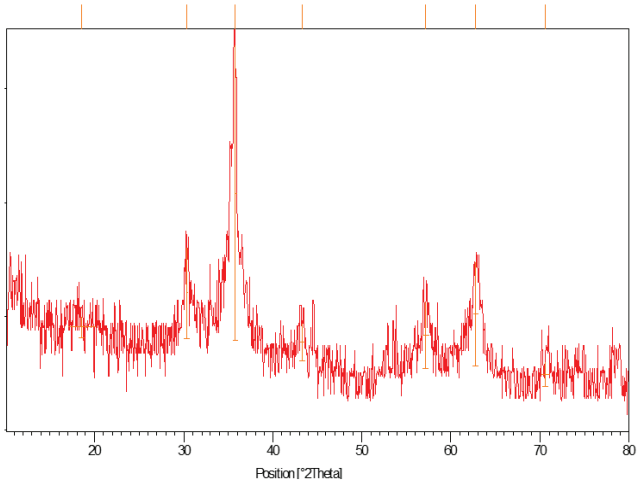

Fig. 4. XRD pattern of synthesized Fe_3O_4 nanoparticles.

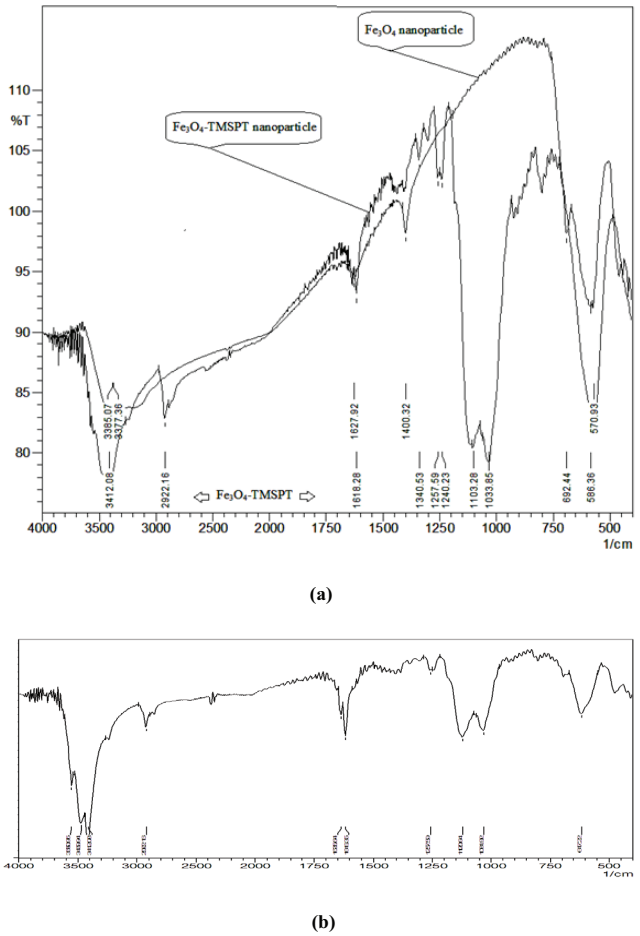

Fig. 5. Infrared spectrum of (a) the prepared Fe_3O_4 and Fe_3O_4–TMSPT MNPs and (b) Fe_3O_4–TMSPT nanoparticles modified with CTAB.

3.3. Effect of coated CTAB amount on adsorption

Fig. 7 shows the yield of 2,4-D removal as a function of the added CTAB to the magnetic particles during their coating. Upon increasing the CTAB concentration, the hydrophobic properties of the surfactant admicelles were dominative on the surface of Fe_3O_4–TMSPT MNPs, and therefore, the surface positive charge increases. At this condition, particularly with regard to pH of sample, the anionic 2,4-D could be adsorbed on the surface of Fe_3O_4–TMSPT MNPs by electrostatic interactions. Furthermore, addition of CTAB under CMC concentration (i.e., 1 mM at 25°C) could facilitate the collection of the MNPs via magnet. As seen in Fig. 7,

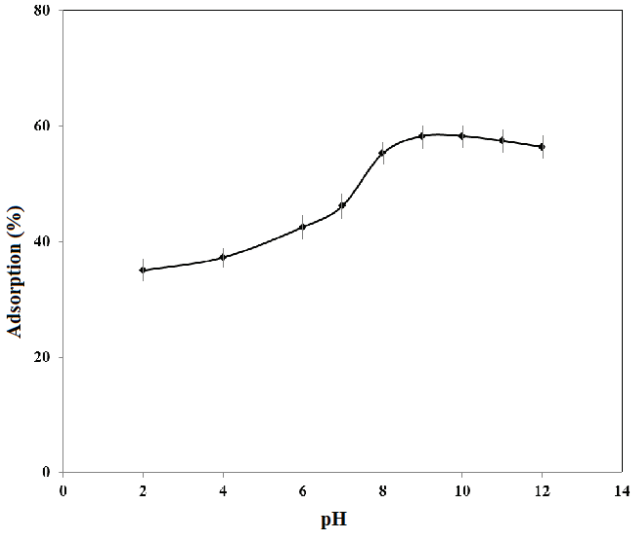

Fig. 6. Effect of pH on 2,4-D adsorption procedure: 2,4-D concentration – 33 ppm, Fe_2O_3 MNP amount – 0.18 g, CTAB amount – 65 ppm, NaCl salt amount – 0.01 M, temperature – 20°C, and time – 10 min.

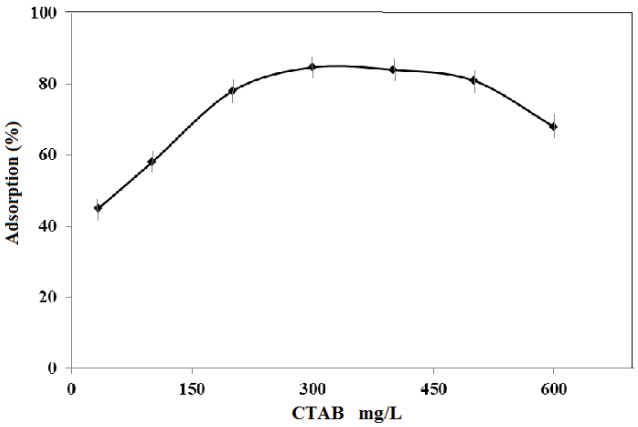

Fig. 7. Effect of CTAB concentration on the yield of 2,4-D adsorption.

the amount of adsorbed 2,4-D increases with the increase in the amount of CTAB and achieves to its maximum value at CTAB amount of 300 mg mL^{-1}. This increase in the adsorption may be due to the gradual formation of CTAB aggregates (hemimicelles, mixed hemimicelles, or admicelles) on the surface of Fe_3O_4–TMSPT MNPs, which enhances the adsorption of 2,4-D gradually. Meantime, the adsorption of 2,4-D at higher CTAB concentrations decreased gradually due to the formation of CTAB aggregates in the solution.

3.4. Effects of ionic strength, temperature, and contact time on adsorption

Table 1 introduces the optimum conditions of ionic strength, temperature, and contact time. The effect of ionic strength on the removal of the 2,4-D (at optimum conditions of the previously mentioned parameters) was studied by addition of NaCl in the concentration range of 0.01–0.2 M. The results of this study showed that at concentration lower than 0.02 M of NaCl, 2,4-D has maximum absorbance, while increasing its concentration leads to significant decrease in its adsorption on the surface of Fe_3O_4–TMSPT MNPs. This behavior could be concerned of the electrostatic interaction of 2,4-D and CTAB during the process, while at the higher concentration of NaCl salt, the electrostatic interference of Na^+ and Cl^- leads to the lower 2,4-D removal efficiency. Thus, 0.01 M of NaCl salt was chosen as optimum concentration for further works.

Due to the presence of surfactant on coated MNPs in the adsorption process, temperature plays an important role on 2,4-D removal. The influence of this parameter was investigated in the range of 15°C–80°C at the optimum conditions of previous factors. The results showed that at the temperatures higher than 20°C, the efficiency of 2,4-D adsorption extremely decreased by increasing the temperature, and at 80°C it is near to the zero. This trend was observed because increasing temperature decreases interactions between the 2,4-D and surfactant molecules, which lead to the remarkable loss of adsorption. Therefore, temperature of 20°C was selected as optimum for the efficient removal of 2,4-D.

The effect of treatment time on the yield of 2,4-D removal by CTAB-coated MNPs has been investigated in a range of 2–160 min. The results showed that the adsorption increased with enhancing the contact time up to 30 min, while it kept constant at the longer time. In other word, the maximum removal could be attained during 30 min. For this reason, 30 min was selected as the optimum contact time.

3.5. Determining maximum capacity of sorbent for 2,4-D removal

In order to determine the maximum capacity of the MNPs adsorbent, at the optimal working conditions, a definite amount of 2,4-D solution (200 ppm) was interacted with different amounts of the adsorbent. The resulted yields of adsorption vs. mass of the adsorbent are plotted in Fig. 8. Maximum adsorbent capacity might be calculated by considering extrapolated point of two lines using the following formula:

$$\text{Adsorbant Capacity}\left(\frac{mg}{g}\right)=\left(\frac{W_{2,4D}(mg)}{W_{MNPex}(g)}\right)\times RR \quad (3)$$

where $W_{2,4\text{-D}}$ and W_{MNPex} are, respectively, the mass of 2,4-D (mg) and Fe_3O_4–TMSPT MNPs (mg g^{-1}) obtained from the extrapolation of the adsorption diagram. Also, RR is the relative amount of adsorbed 2,4-D at optimum conditions. Accordingly, the maximum capacity of Fe_3O_4–TMSPT MNPs as the adsorbent was calculated as 4.9 mg g^{-1}.

Table 1
Optimum conditions of ionic strength, temperature, and contact time for 2,4-D removal

Parameters	Studied range	Optimum amount
Ionic strength	0.01–0.2 M	0.01 M
Temperature	15°C–80°C	20°C
Contact time	2–160 min	30 min

3.6. 2,4-D desorption and reusability of the sorbents

Since 2,4-D adsorption on the Fe_3O_4 MNPs modified with CTAB is a reversible process, regeneration or activation of Fe_3O_4 MNPs is possible to reuse them [32]. Desorption of the 2,4-D from the magnetic adsorbents was examined using different solvents. It was found that the 2,4-D could be efficiently desorbed from the magnetic sorbents by rinsing the sorbent with 0.05 M HCl solution for three times.

The results showed that a desorption efficiency higher than 90% could be achieved during a short time of about 3 min. Further studies showed that Fe_3O_4 MNPs modified with CTAB could be regenerated and reused for at least three successive removal processes. Under higher removal cycles, the efficiency of removal decreases due to the dissolving and/or losing some amounts of CTAB during the successive steps.

3.7. Results of mathematical modeling and kinetic studies

Fig. 9 presents the experimental aqueous-phase adsorption isotherms for 2,4-D/Fe_3O_4 MNPs modified with CTAB system along with the curve fitted by different isotherm models. Meanwhile, the resulted isotherm parameters and the values of Chi-square are also given in Table 2. Considering

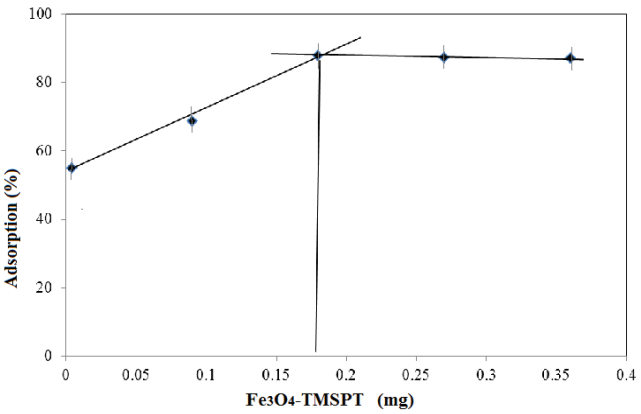

Fig. 8. Yield of 2,4-D adsorption versus amount of Fe_3O_4–TMSPT MNPs.

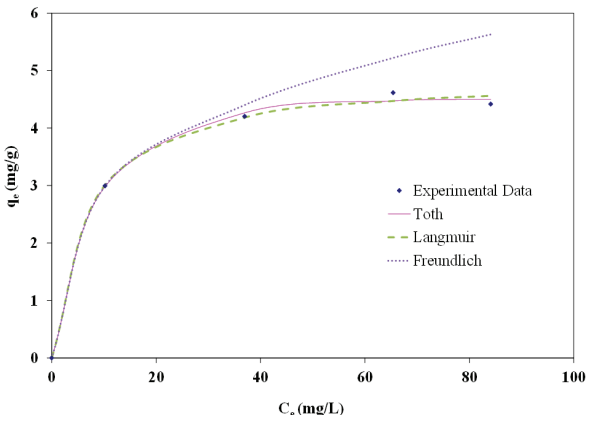

Fig. 9. Langmuir, Freundlich, and Toth isotherms for the adsorption of 2,4-D on Fe_3O_4 MNPs modified with CTAB.

Table 2
Parameters of the isotherm models for the adsorption of 2,4-D onto onto Fe_3O_4 magnetic nanoparticles modified with CTAB

Model	Equation	Parameter	Value	χ^2
Toth	$q_e = \frac{K_t C_e}{(a_t + C_e)^{1/t}}$	K_t	8.231	0.007
		a_t	10.153	
		$1/t$	1.107	
Langmuir	$q_e = \frac{q_m K_a C_e}{1 + K_a C_e}$	q_m	4.910	0.009
		K_a	0.156	
Freundlich	$q_e = K_F C_e^{1/n}$	K_F	1.493	0.103
		$1/n$	0.299	

the isotherm plots (Fig. 9) exhibits that Toth and Langmuir isotherms more accurately describe the sorption behavior of 2,4-D. The used method for deriving the isotherm parameters diminishes the Chi-square statistic, and the results showed that the Toth and Langmuir isotherms exhibit lower values and hence a better fit. The adsorption data obeyed the Langmuir and Toth models exhibiting heterogeneous surface conditions and monolayer adsorption. In other words, 2,4-D as the adsorbate has a high affinity for the surface at low surface coverage. However, by increasing the coverage, the affinity of the adsorbate to the surface decreases.

To evaluate the adsorption kinetic of 2,4-D, the effect of exposure time on the adsorption yield was studied (Table 3). Then, pseudo-first-order and pseudo-second-order kinetic models were examined. The non-linear Chi-square statistic was utilized to explain the conformity between experimental data and the model-predicted values. Meantime, the Lagergren pseudo-first-order kinetic model is expressed as Eq. (4) [33]:

$$q_t = q_e - q_e 10^{\frac{-k_1 t}{2.303}} \quad (4)$$

where q_t and q_e are, respectively, the amount of 2,4-D adsorbed (mg g^{-1}) at any time and equilibrium time, while k_1 represents

Table 3
The values of Chi-square statistic and rate constants for the pseudo-first-order and pseudo-second-order models

Model	Parameter	Value
Pseudo-first-order	k_1	0.331
	q_e	2.323
	χ^2	0.031
Pseudo-second-order	k_2	0.297
	q_e	2.372
	χ^2	0.019

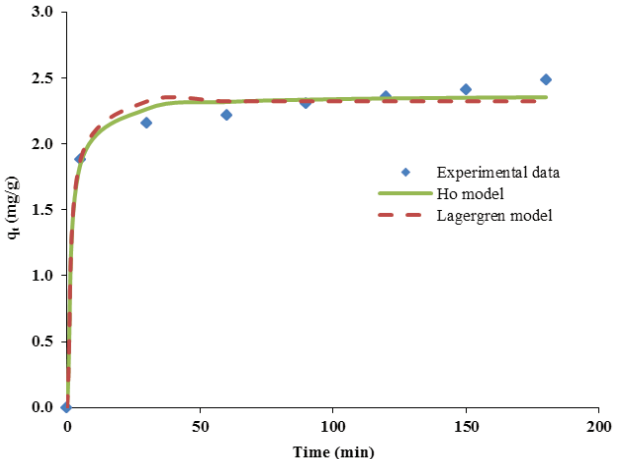

Fig. 10. Comparison of the experimental data with the model-predicted (Lagergren and Ho) values corresponding to the adsorption of 2,4-D on Fe_3O_4 MNPs modified with CTAB.

the rate constant in min^{-1}. On the other hand, the Ho pseudo-second-order rate equation is described as Eq. (5) [34]:

$$q_t = \frac{q_e^2 k_2 t}{q_e k_2 t + 1} \quad (5)$$

where k_2 corresponds to the rate constant of pseudo-second-order model (g mg^{-1} min^{-1}). Fig. 10 presents the results of fitting of the experimental data with the model-predicted (Lagergren and Ho) values. Meantime, Table 3 shows the values of Chi-square statistic and rate constants for the pseudo-first-order and pseudo-second-order models. As seen, the value of Chi-square statistic for the second-order model is lower than the corresponding value for the pseudo-first-order model. These results confirm that the pseudo-second-order equation of Ho could appropriately fit over the wide range of contact times and describe the kinetic of 2,4-D sorption onto Fe_3O_4 MNPs modified with CTAB [35].

4. Conclusion

2,4-D as a herbicide was successfully removed from aqueous solution by the aid of surface-modified MNPs. Fe_3O_4–TMSPT MNPs were prepared, and their surface was modified by CTAB. The removal process variables were investigated and optimized. The results of process optimization showed that

CTAB-coated Fe_3O_4–TMSPT MNPs could efficiently remove 2,4-D from water at the following operation conditions: pH 9, temperature of 20°C, CTAB amount of 300 mg mL^{-1}, salt amount of 0.01 M, and contact time of 30 min. The maximum capacity of the adsorbent at optimal conditions was calculated as 4.9 mg g^{-1}. Meanwhile, the kinetic of 2,4-D adsorption obeyed the pseudo-second-order model.

References

[1] H. Kidd, D.R. James, The Agrochemicals Handbook, The Royal Society of Chemistry, Cambridge, England, 1991.

[2] N.H. Nelson, S.D. Faust, Acidic dissociation constants of selected aquatic herbicides, Environ. Sci. Technol., 3 (1969) 1186–1188.

[3] A.D. Carter, Herbicide movement in soils: principles, pathways and processes, Weed Res., 40 (2000) 113–122.

[4] WHO, 2,4-D in Drinking-water, Background Document for Preparation of WHO Guidelines for Drinking-water Quality, WHO/SDE/WSH/03.04/70, World Health Organization, Geneva, 2003.

[5] D.J. Hamilton, A. Ambrus, R.M. Dieterle, A.S. Felsot, C.A. Harris, P.T. Holland, A. Katayama, N. Kurihara, J. Linders, J. Unsworth, S.S. Wong, Regulatory limits for pesticide residues in water, Pure Appl. Chem., 75 (2003) 1123–1155.

[6] M. Rahimi-Nasrabadi, R. Akhoondi, S.M. Pourmortazavi, F. Ahmadi, Predicting adsorption of aromatic compounds by carbon nanotubes based on quantitative structure property relationship principles, J. Mol. Struct., 1099 (2015) 510–515.

[7] H. El Harmoudi, L. El Gaini, E. Daoudi, M. Rhazi, Y. Boughaleb, M.A. El Mhammedi, A. Migalska-Zalas, M. Bakasse, Removal of 2,4-D from aqueous solutions by adsorption processes using two biopolymers: chitin and chitosan and their optical properties, Opt. Mater., 36 (2014) 1471–1477.

[8] B.K. Jung, Z. Hasan, S.H. Jhung, Adsorptive removal of 2,4-dichlorophenoxyacetic acid (2,4-D) from water with a metal–organic framework, Chem. Eng. J., 234 (2013) 99–105.

[9] S. Bakhtiary, M. Shirvani, H. Shariatmadari, Characterization and 2,4-D adsorption of sepiolite nanofibers modified by N-cetylpyridinium cations, Microporous Mesoporous Mater., 168 (2013) 30–36.

[10] E. Ayranci, N. Hoda, Studies on removal of metribuzin, bromacil, 2,4-d and atrazine from water by adsorption on high area carbon cloth, J. Hazard. Mater., 112 (2004) 163–168.

[11] X. Zhang, X. Lu, S. Li, M. Zhong, X. Shi, G. Luo, L. Ding, Investigation of 2,4-dichlorophenoxyacetic acid adsorption onto MIEX resin: optimization using response surface methodology, J. Taiwan Inst. Chem. Eng., 45 (2014) 1835–1841.

[12] K. Nejati, S. Davary, M. Saati, Study of 2,4-dichlorophenoxyacetic acid (2,4-D) removal by Cu-Fe-layered double hydroxide from aqueous solution, Appl. Surf. Sci., 280 (2013) 67–73.

[13] M. Sathishkumar, A.R. Binupriya, D. Kavitha, R. Selvakumar, R. Jayabalan, J.G. Choi, S.E. Yun, Adsorption potential of maize cob carbon for 2,4-dichlorophenol removal from aqueous solutions: equilibrium, kinetics and thermodynamics modeling, Chem. Eng. J., 147 (2009) 265–271.

[14] M.Z. Momčilović, M.S. Ranđelović, A.R. Zarubica, A.E. Onjia, M. Kokunešoski, B.Z. Matović, SBA-15 templated mesoporous carbons for 2,4-dichlorophenoxyacetic acid removal, Chem. Eng. J., 220 (2013) 276–283.

[15] N. Ayar, B. Bilgin, G. Atun, Kinetics and equilibrium studies of the herbicide 2,4-dichlorophenoxyacetic acid adsorption on bituminous shale, Chem. Eng. J., 138 (2008) 239–248.

[16] S.M. Pourmortazavi, S.S. Hajimirsadeghi, Application of supercritical carbon dioxide in energetic materials processes: a review, Ind. Eng. Chem. Res., 44 (2005) 6523–6533.

[17] S.M. Pourmortazavi, I. Kohsari, S.S. Hajimirsadeghi, Electrosynthesis and thermal characterization of basic copper carbonate nanoparticles, Cent. Eur. J. Chem., 7 (2009) 74–78.

[18] S.M. Pourmortazavi, S.S. Hajimirsadeghi, M. Rahimi-Nasrabadi, I. Kohsari, Optimization of parameters for the synthesis of silver iodate submicron belts by Taguchi robust design method, Chem. Eng. Commun., 198 (2011) 1182–1188.

[19] M. Shamsipur, S.M. Pourmortazavi, S.S. Hajimirsadeghi, M. Roushani, Applying Taguchi robust design to the optimization of synthesis of barium carbonate nanorods via direct precipitation, Colloids Surf., A, 423 (2013) 35–41.

[20] S.M. Pourmortazavi, S.S. Hajimirsadeghi, I. Kohsari, R. Fareghi Alamdari, M. Rahimi-Nasrabadi, Determination of the optimal conditions for synthesis of silver oxalate nanorods, Chem. Eng. Technol., 31 (2008) 1532–1535.

[21] M. Sadeghi, M. Irandoust, F. Khorshidi, M. Feyzi, F. Jafari, T. Shojaeimehr, M. Shamsipur, Removal of Arsenic (III) from natural contaminated water using magnetic nanocomposite: kinetics and isotherm studies, J. Iran Chem. Soc., 13 (2016) 1175–1188.

[22] F. Ge, H. Ye, M.-M. Li, B.-X. Zhao, Efficient removal of cationic dyes from aqueous solution by polymer-modified magnetic nanoparticles, Chem. Eng. J., 198–199 (2012) 11–17.

[23] C. Huang, B. Hu, Silica-coated magnetic nanoparticles modified with γ-mercaptopropyl trimethoxysilane for fast and selective solid phase extraction of trace amounts of Cd, Cu, Hg, and Pb in environmental and biological samples prior to their determination by inductively coupled plasma mass spectrometry, Spectrochim. Acta, Part B, 63 (2008) 437–444.

[24] M. Faraji, Y. Yamini, A. Saleh, M. Rezaee, M. Ghambarian, R. Hassani, A nanoparticle-based solid-phase extraction procedure followed by flow injection inductively coupled plasma-optical emission spectrometry to determine some heavy metal ions in water samples, Anal. Chim. Acta, 659 (2010) 172–177.

[25] Q. Wu, G. Zhao, C. Feng, C. Wang, Z. Wang, Preparation of a graphene-based magnetic nanocomposite for the extraction of carbamate pesticides from environmental water samples, J. Chromatogr. A, 1218 (2011) 7936–7942.

[26] G. Zhao, S. Song, C. Wang, Q. Wu, Z. Wang, Determination of triazine herbicides in environmental water samples by high-performance liquid chromatography using graphene-coated magnetic nanoparticles as adsorbent, Anal. Chim. Acta, 708 (2011) 155–159.

[27] P. Li, D.E. Miser, S. Rabiei, R.T. Yadav, M.R. Hajaligol, The removal of carbon monoxide by iron oxide nanoparticles, Appl. Catal., B, 43 (2003) 151–162.

[28] M.H. Mashhadizadeh, Z. Karami, Solid phase extraction of trace amounts of Ag, Cd, Cu, and Zn in environmental samples using magnetic nanoparticles coated by 3-(trimethoxysilyl)-1-propantiol and modified with 2-amino-5-mercapto-1,3,4-thiadiazole and their determination by ICP-OES, J. Hazard. Mater., 190 (2011) 1023–1029.

[29] M. Taghdiri, N. Zamani, Hexamine adsorption study on activated carbon from aqueous solutions for application in treatment of hexamine industrial wastewater, Int. J. Environ. Sci. Technol., 10 (2013) 19–26.

[30] M. Rahimi-Nasrabadi, S.M. Pourmortazavi, M.R. Ganjali, S.S. Hajimirsadeghi, M.M. Zahedi, Electrosynthesis and characterization of zinc tungstate nanoparticles, J. Mol. Struct., 1047 (2013) 31–36.

[31] S.M. Pourmortazavi, M. Rahimi-Nasrabadi, M. Khalilian-Shalamzari, H.R. Ghaeni, S.S. Hajimirsadeghi, Facile chemical synthesis and characterization of copper tungstate nanoparticles, J. Inorg. Organomet. Polym., 24 (2014) 333–339.

[32] C. Wang, C. Feng, Y. Gao, X. Ma, Q. Wu, Z. Wang, Preparation of a graphene-based magnetic nanocomposite for the removal of an organic dye from aqueous solution, Chem. Eng. J., 173 (2011) 92–97.

[33] G. Annadurai, R.S. Juang, D.J. Lee, Use of cellulose-based wastes for adsorption of dyes from aqueous solutions, J. Hazard. Mater., 92 (2002) 263–274.

[34] S. Sohrabnezhad, A. Habibi-Yangjeh, S. Eftekhari, Nanodimensional AlMCM-41 material for adsorption of dyes: thermodynamic and kinetic studies, Int. J. Nano Dimens., 4 (2013) 91–104.

[35] T. Madrakian, A. Afkhami, H. Mahmood-Kashani, M. Ahmadi, Adsorption of some cationic and anionic dyes on magnetite nanoparticles-modified activated carbon from aqueous solutions: equilibrium and kinetics study, J. Iran. Chem. Soc., 10 (2013) 481–489.